Neuro-Oncology
27(5), 1241–1255, 2025 | https://doi.org/10.1093/neuonc/noae282 | Advance Access date 28 December 2024

Therapeutic effect of novel drug candidate, PRG-N-01, on NF2 syndrome-related tumor

Yeon-Ho Chung[†], Soyoung Park[†], Moonyoung Lee, Jongwon Lee, Yeongseon Ji, Yi Jin Song, Tae-Gyun Woo, Eunbyeol Shin, Songyoung Baek, Young Jun Hwang, Yuju Kim, Minju Kim, Jin Han, Hong-Rae Kim, Jungmin Choi, Bae-Hoon Kim, and Bum-Joon Park

All author affiliations are listed at the end of the article

[†]These authors contributed equally to this work.

Corresponding Authors: Bum-Joon Park, PhD, College of Natural Science, Pusan National University, Busan, Republic of Korea (bjpark1219@pusan.ac.kr); Bae-Hoon Kim, PhD, Rare Disease R&D Center, PRG S&T Co., Ltd, Busan, Republic of Korea (bk728@prgst.com).

Abstract

Background. NF2-related schwannomatosis (NF2-SWN) is associated with multiple benign tumors in the nervous system. NF2-SWN, caused by mutations in the NF2 gene, has developed into intracranial and spinal schwannomas. Because of the high surgical risk and frequent recurrence of multiple tumors, targeted therapy is necessary. However, there are no approved drugs.

Methods. We examined the action mechanism of PRG-N-01, a candidate molecule for NF2-SWN, through the direct binding assay and mass spectrometry. For in vitro anti-proliferative experiments, primary cells derived from the NF2 mouse model and patient tumors were treated with PRG-N-01. The in vivo therapeutic and preventive efficacy was validated via intraperitoneal and oral administration in the NF2 mouse model (Postn-Cre; Nf2f/f). Gene expression profile in the DRG of the mouse model was explored by RNA sequencing. The pharmacological properties of PRG-N-01 were analyzed through the preclinical study.

Results. PRG-N-01 binds to the N-terminal extremity of TGFβR1 (TβR1) kinase domain, where TβR1 and RKIP interact, inhibiting the binding and preventing degradation of RKIP. In vivo administration in the mouse model suppressed schwannoma progression in the DRG. Early oral administration of the PRG-N-01 also demonstrated preventive effects on NF2-SWN. PRG-N-01 treatment suppressed tumor growth genes while upregulating genes related to for normal cell metabolism and Schwann cell differentiation in DRG. PRG-N-01 showed druggable properties through the preclinical study, including ADME, pharmacodynamics, pharmacokinetics, and toxicology.

Conclusions. Together, our study provides the rationale and critical data for a prospective clinical trial of PRG-N-01 in NF2-SWN patients indicating PRG-N-01 as a promising candidate for the treatment.

Key Points

- PRG-N-01 binds to the 230-322 aa of TβR1, where TβR1 and RKIP interact, and it prevents unnecessary degradation of RKIP without hampering the TGF-β signaling.
- PRG-N-01 shows the therapeutic and preventive efficacy in the NF2 mouse model (*Postn-Cre*; *Nf2*$^{f/f}$) via intraperitoneal and early oral administration and indicates a comparative advantage over other Phase 2 drugs and has promising preclinical data.
- The number of RKIP-positive satellite cells and the number of Schwann cell whorls showed a negative correlation in the DRG.

Graphical Abstract

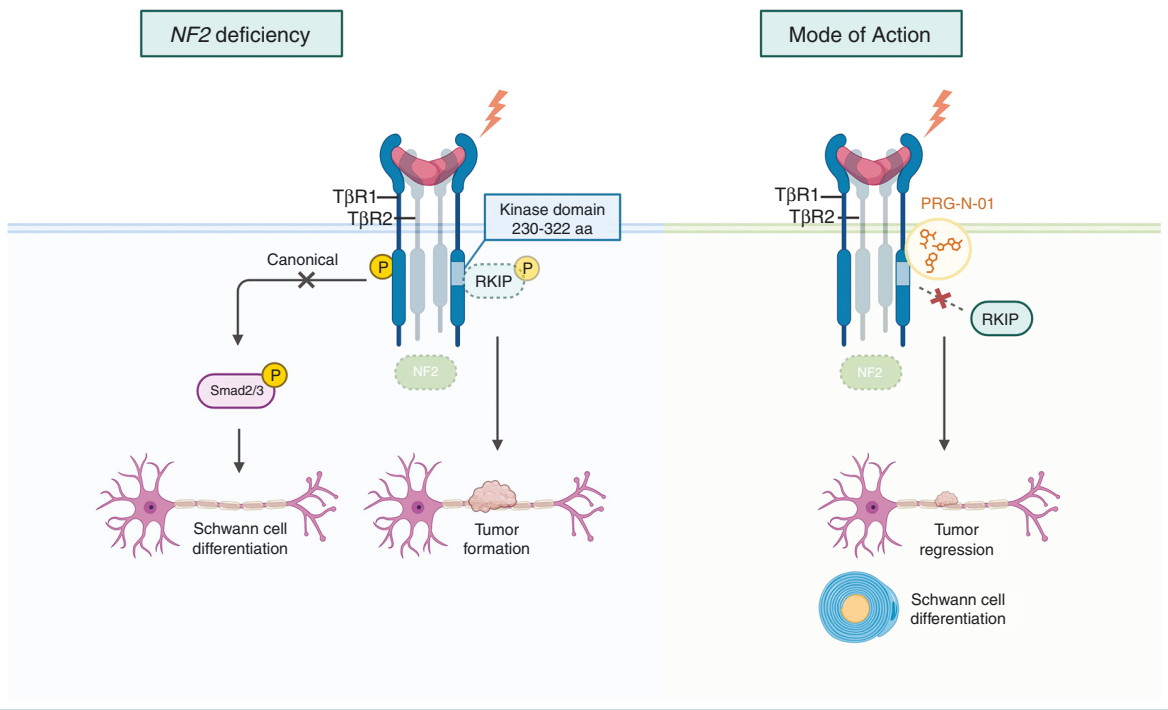

Importance of the Study

This study addresses a critical need in the treatment of NF2-related schwannomatosis (NF2-SWN), a genetic condition marked by the development of multiple benign tumors in the nervous system, which presents high surgical risks and frequent recurrences. Despite the urgent demand for effective therapies, there are currently no approved drugs for this condition. The investigation of PRG-N-01, a novel candidate molecule targeting NF2-SWN, holds significant potential in filling this therapeutic gap. By examining PRG-N-01's binding mechanisms, anti-proliferative effects, and pharmacological properties in both in vitro and in vivo models, this study offers foundational evidence that PRG-N-01 could represent a breakthrough in NF2-SWN treatment. This work not only highlights the promising efficacy of PRG-N-01 but also establishes a basis for advancing toward clinical trials, potentially providing new hope for NF2-SWN patients.

NF2-related schwannomatosis (NF2-SWN) is a rare autosomal dominant genetic disorder, caused by loss-of-function mutations of the *NF2* tumor suppressor gene encoding a protein called Merlin. NF2-SWN is characterized by the growth of multiple tumors in the nervous system, particularly those in the skull and spine[1] and is associated with intracranial and spinal schwannoma, meningioma, and ependymoma.[2] NF2-related tumors are benign, but their high risk of surgical removal and frequent occurrence of multiple recurrent tumors require targeted therapies.[3,4] Unfortunately, there are currently no targeted drugs approved by the FDA to treat NF2-SWN patients. As non-targeted treatment, Bevacizumab, a humanized monoclonal antibody that targets vascular endothelial growth factor A, has been shown to improve hearing and reduce tumor volume in about 40% of patients with progressive NF2-associated vestibular schwannomas (VS).[5] However, the drug's effects are not durable in patients who do respond, and bevacizumab may induce serious adverse effects, such as hypertension and proteinuria, that make long-term treatment difficult for some patients.[6] Clinical phase 2 trials, such as Brigatinib and Selumetinib, are presently in progress to explore the effectiveness of targeted therapies in treating NF2-associated VS, yet the drug's efficacy remains uncertain. Therefore, more effective and safer targeted therapies are urgently needed for NF2-associated tumors.

Merlin, a product of the *NF2* gene, is a cell membrane protein that mediates contact-dependent inhibition of proliferation as a tumor suppressor.[6] Loss of function of Merlin results in deregulation of numerous signaling pathways involved in tumorigenesis, including the Hippo pathway, Raf/MEK/ERK, PI3K/Akt, and mTOR signaling pathways.[7–10] Raf-kinase inhibitor protein (RKIP) has been identified as

a negative regulator of the Raf-MEK-ERK pathway and is an important negative modulator of the PI3Kinase/Akt and mTOR signaling pathways involved in various biological processes, such as cell proliferation and differentiation.[11–13] Low or loss of RKIP expression is associated with tumor cell survival, proliferation, and metastasis in numerous human cancers, indicating that RKIP is an endogenous tumor suppressor protein.[14–16]

Our previous study demonstrated that physical contact-induced reduction of RKIP leads to Merlin instability, resulting in tumorigenic progression in mesothelioma.[17] Based on these findings, a novel pathomechanism of NF2-SWN was identified: Merlin deficiency decreases the stability of transforming growth factor-beta receptor 2 (TβR2), and physical stimuli such as pressure or heavy materials induce unnecessary interaction between transforming growth factor-beta receptor 1 (TβR1) and RKIP. This neo-interaction results in the phosphorylation and degradation of RKIP. RKIP reduction consequently mediates MAPK activation as well as Snail-mediated p53 suppression and occurrence of EMT in *NF2*-deficient cells.[18] To obtain drugs that ameliorate this new NF2-SWN pathology, we screened candidate chemicals that selectively inhibit the aberrant interaction between TβR1 and RKIP, which induces a reduction of RKIP. A novel chemical, Nf18001, was selected finally and it inhibited proliferation and promoted differentiation of HEI-193 human schwannoma cells, and suppressed tumor growth in an allograft model without interfering with canonical TGF-β signaling.[19]

Here, we present a report on the biological characteristics of orally bioavailable PRG-N-01 (new code name of Nf18001). PRG-N-01 binds to the TβR1 kinase domain and inhibits the direct interaction between TβR1 and RKIP. In vivo administration of PRG-N-01 showed therapeutic and preventive effects by reducing the incidence of multiple sporadic tumorigenesis in NF2 model mice and inhibiting the development of schwannomas in the dorsal root ganglion (DRG). Additionally, DRG transcriptome analysis revealed that PRG-N-01 treatment decreased the cell division pathway and increased the oxidative phosphorylation pathway in tumor tissue. Furthermore, PRG-N-01 exhibited reasonable pharmacological properties as a drug in preclinical studies.

Materials and Methods

Mice

All experimental procedures involving laboratory animals were approved by the Animal Care Committee of Pusan National University (Approval number, PNU-2023-0113). NF2 (FVB/NJ) mice were obtained from Dr. D.W. Clapp (Indiana University, Indianapolis, IN). FVB/NJ mice were obtained from The Jackson Laboratory. See Supplementary Materials for details.

Image Acquisition of [18F] FDG PET/CT

Micro-PET images were acquired using an Inveon PET/CT scanner (Siemens Healthcare). [18F] FDG (580 ± 30 μCi) was administered intravenously through the tail vein. All of the micro-PET images were reconstructed using a 2-dimensional ordered-subset expectation maximum (OSEM) algorithm, and focal accumulations in the microPET images were quantified by region of interest analysis. Signal-to-background ratios were calculated using average counts per voxel on the coronal images.

Tumor Volume Quantitation

Tissue processing and quantification of dorsal root ganglion (DRG) volume were performed following previously established methods [21]. Spines were fixed with tissue fixative and then decalcified using 5% formic acid. DRGs and spinal nerves were meticulously isolated under a dissecting microscope (ZEISS Stemi 508). Tumor volume was determined by capturing DRG images with a microscope camera (ZEISS Axiocam 208). The tumor volume was calculated using the formula: volume = length × width × 0.52, where length and width measurements approximated the dimensions of a specific spheroid-shaped tumor.

Protein–Protein Interaction Analyses

GST-pull down assay and immunoprecipitation assays were performed to evaluate protein–protein interactions. For GST pull-down assay, agarose-bead–conjugated GST–TβR1 kinase domain aa 148-503 (KD) recombinant protein was incubated with HA-tagged RKIP- or FLAG-tagged Smad-2 or Smad3-transfected HEK 293 cell lysates or HA-tagged TβR2-transfected HCT116 cell lysates in PBS for overnight at 4°C. To evaluate the RKIP-MEK1/2 interaction, agarose-bead-conjugated GST-RKIP recombinant protein was incubated with HEK 293 cell lysates. For the immunoprecipitation assay, FLAG-tagged c-Raf or HA-tagged RKIP-transfected HEK 293 cell lysates in PBS were used. Whole lysates were incubated with appropriate primary antibodies overnight at 4°C and reacted with agarose-bead–conjugated protein A/G (Invitrogen) for 2 h. After centrifugation, the precipitates were washed twice with RIPA buffer and subjected to SDS-PAGE and western blotting analysis.

LC-MS/MS Analysis

The LC-MS/MS analysis was performed on a Waters UPLC Acquity I class plus coupled to a Qtrap 6500 plus (Applied Biosystems/Sciex). A Phenomenex, Aeris, 3.6 μm, 100×2.1 mm column was used for separation. The MS system was controlled by Analyst 1.6.1 software. See Supplementary Materials for details.

Prediction of TβR1-RKIP Complex and Molecular Docking

The amino acid sequences of the cytoplasmic domain (148-503) of TβR1 (P36897-1, Length 503) and the full-length RKIP (A0A1C6YP47, Length 190) were submitted as separate chains to the ColabFold (56) v1.5.2 (AlphaFold2 using MMseq2) using the default settings and the

homodimer options: msa_mode = mmseq2_uniref_env, pair_mode = unpaired_paired, model_type = auto, num_recycles = auto, recycle_early_stop_tolerance = auto, max_msa = auto, num_seeds = 1. Predicted structures with best-ranked model 1 were selected for further analysis and visualized using Schrödinger Maestro software. Molecular docking experiments were performed using Schrödinger Glide software (version 2022-4). The predicted TβR1-RKIP model generated from ColabFold was imported to Maestro, and the protein was prepared for docking using the Protein Preparation Workflow with the OPL4 force field. The TβR1 portion was isolated, and the receptor grid for docking was defined as the centroid of 250Q, 251T, 255R, 265A with length 20A. PRG-N-01 was imported to Maestro in a SMILES format, and the compound was prepared for docking using the LigPrep module, which generated all possible states at a target pH of 7.0 ± 2.0. The prepared compounds were docked to the protein structure using the Glide software with extra precision (XP) settings.

For detailed methodologies of Western blotting analysis, histology and immunohistochemistry, bulk RNA sequencing, preclinical study, and so on, see Supplementary Materials.

Statistical Analysis

Statistical differences were assessed using the Student's *t*-test or 1-way ANOVAs combined with the Dunnett's test for multiple comparisons (GraphPad Prism software, version 9.5.1). *P*-values < .05 were considered significant.

Results

Identification of the TGFβR1 Binding Site for RKIP

Previously, we reported that *NF2* deficiency decreases the stability of TβR2 and induces unnecessary interaction between TβR1 and RKIP.[18,19] This interaction induces phosphorylation and degradation of RKIP. Considering that the decomposition of RKIP is influenced by the catalytic activation of TβR1,[18,19] it is expected that RKIP would bind to the kinase domain of TβR1. Therefore, TβR1 kinase domain (148-503) and RKIP recombinant protein were produced and GST-pulldown assay was conducted (**Figure 1A**). As shown in **Figure 1B**, RKIP binds to the kinase domain of TβR1 directly. To identify the more specific region responsible for the TβR1-RKIP interaction, we performed further pulldown assay using various TβR1 fragments (**Figure 1A**). RKIP strongly binds specifically to the N-terminal extremity of TβR1 kinase domain (230-322) (**Figure 1C**). Through in silico molecular docking analysis, 6 residues (225R, 250Q, 251T, 255R, 265A, and 323T) in TβR1 230-322 region, were estimated to have hydrogen bonds less than 1Å distance with RKIP (**Figure 1D and Supplementary Figure 1A**). Consequently, the docking grid was generated centered around 250Q, 251T, 255R, and 265A of TβR1. Using mutants that substituted the specified residues, in vitro binding assay was conducted, revealing that A265 could be a critical residue of TβR1 for binding to RKIP (**Figure 1E**). Our result demonstrated that there is the neo-protein-protein interaction between the TβR1 kinase domain and RKIP. Therefore, it is essential to verify whether our drug, which inhibits the binding of TβR1 and RKIP, targets this specific binding site to enhance target accuracy, maximize therapeutic effects, and minimize side effects.

PRG-N-01 Selectively Inhibits the Interaction Between TβR1 and RKIP by Specifically Binding to the TβR1 kinase domain

As it had been demonstrated that the binding of a small molecule to the proteins affects the integrity of the protein–protein interaction through conformational changes or competes with the original protein partner,[20] we explore the binding mode of PRG-N-01 to TβR1-RKIP complex. To confirm that PRG-N-01 inhibits the interaction of TβR1 and RKIP through precise binding region, in vitro binding assays were performed using TβR1 kinase domain recombinant protein. PRG-N-01 interrupted the interaction of TβR1 kinase domain (148-503) and RKIP directly (**Figure 2A and B**). In addition, PRG-N-01 also inhibited interaction at a more precise binding site of TβR1 (230-322) and RKIP identified in Figure 1C (**Figure 2C**). To validate the accurate target of PRN-N-01 in the TβR1-RKIP complex, using LC-MS/MS analysis, in vitro binding assay between PRG-N-01 and recombinant proteins (GST-TβR1 kinase domain and GST-RKIP) was performed. The LC-MS/MS analysis showed that PRG- N-01 has an affinity for the TβR1 kinase domain, but not for the GST alone and GST-RKIP (**Figure 2D and E**). To explore the plausible binding mode of PRG-N-01 and gain further insight into how it can interfere with RKIP binding to TβR1, we conducted in silico molecular docking analysis. The molecular docking experiment yielded a plausible binding mode of PRG-N-01 to TβR1. The primary amine of the PRG-N-01 formed 2 hydrogen bonding interactions with the backbones of 250Q and 252V, and it was further stabilized with a pi-cation interaction between the central triazole and 255R (**Figure 2F and Supplementary Figure 1B**). In in vitro binding assays, PRG-N-01 did not inhibit the binding of the TβR1 R255A mutant to RKIP, in contrast to its successful inhibition of the interaction between the TβR1 WT and RKIP. Moreover, the binding of the TβR1 T251A mutant to RKIP was inhibited partially by PRG-N-01. These findings suggest that the residues Thr251 and Arg255 of TβR1 could be critical sites for the binding of PRG-N-01 to TβR1 (**Figure 2G**). Accordingly, our results underscore that the neo-protein-protein interaction between the TβR1 kinase domain and RKIP could be a target site for the treatment inhibiting tumor formation under *NF2* deficient conditions.[21]

In the TGF-β signaling pathway, upon binding of the activated TGF-β ligand to TβR2, it recruits and activates TβR1,[22,23] which subsequently activates downstream mediators Smad2 and Smad3.[24,25] To evaluate the specificity of the PRG-N-01, we investigated the effect of PRG-N-01 on the interaction between TβR1 and its binding partners including TβR2, Smad2, and Smad3. We observed that PRG-N-01 had no appreciable effects on the interaction of TβR1-TβR2 (**Supplementary Figure 2A**), TβR1-Smad2 (**Supplementary Figure 2B**), and TβR1-Smad3 (**Supplementary Figure 2B**). Furthermore, PRG-N-01 did

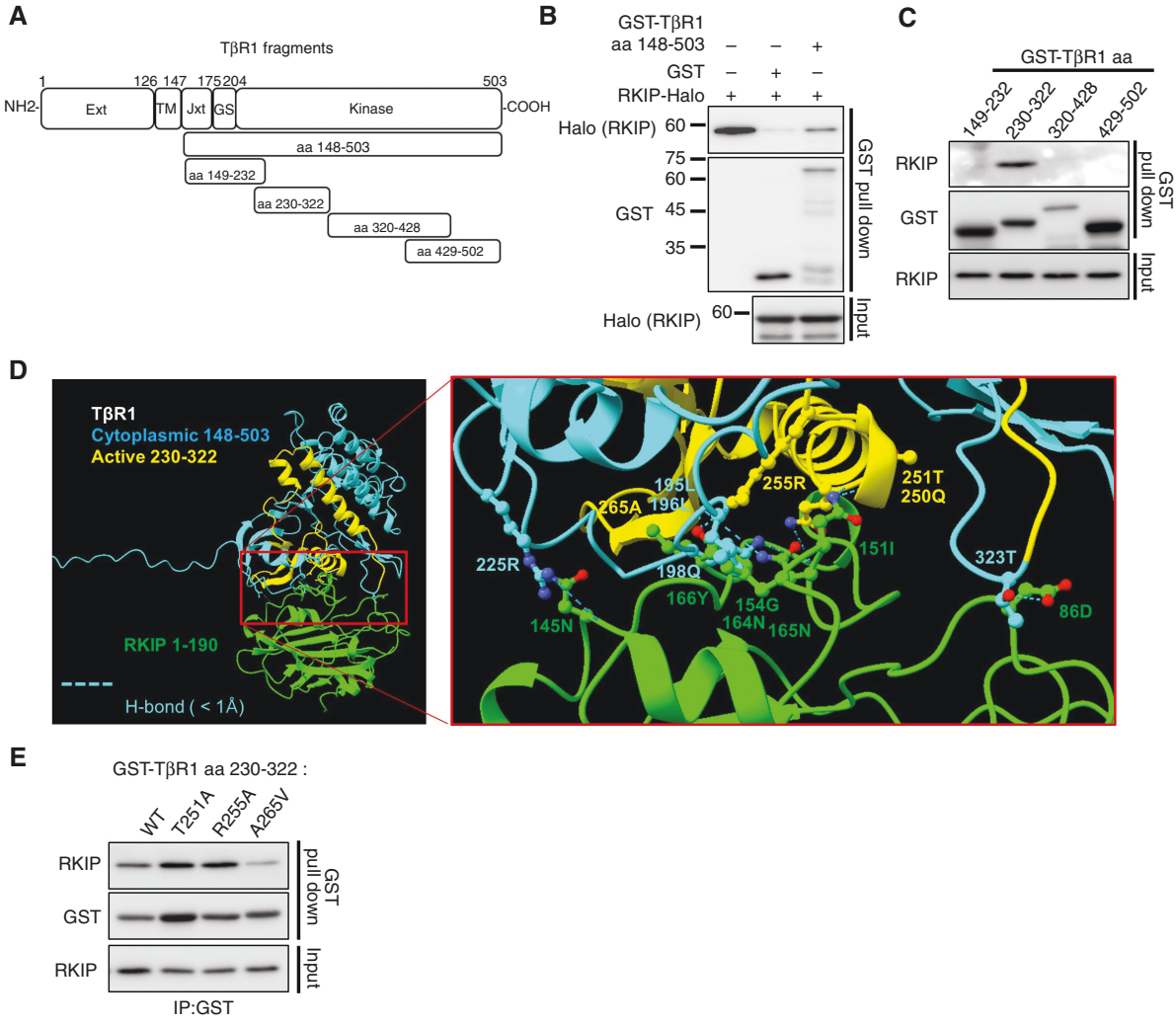

Figure 1. **Identification of the essential binding domain between RKIP and TβR1. (A)** TβR1 fragments used in these studies. The full-length structure of TβR1 is shown for reference. Ext; extracellular ligand-binding domain, TM; Transmembrane domain, GS; GS region of TβR1. **(B)** In vitro TβR1 kinase domain (aa148-503)-RKIP binding assay. **(C)** Purified GST-tagged TβR1 KD deletion mutants were tested for binding to purified RKIP. (D) In silico molecular docking analysis of RKIP and TβR1 cytoplasmic (148-503) or active (230-322) region (E) In vitro binding of RKIP with GST-tagged TbR1 WT (aa 230-322) or various mutants.

not affect the interaction between RKIP, a physiological endogenous inhibitor of the Raf-1/MEK/ERK pathway,[26] with MEK1/2 (**Supplementary Figure 2C**) and c-Raf (**Supplementary Figure 2D**). These results underscore that PRG-N-01 selectively targets the TβR1-RKIP interaction but no other interactions involving major partners that interact with TβR1 or RKIP. There is a concern that PRG-N-01 may affect the kinase activity of TβR1 due to its binding to the TβR1 kinase domain. However, it is suggested that PRG-N-01 does not directly affect the kinase active site at lysine 232,[21] but rather binds around the active site (**Figure 2F and Supplementary Figure 1B**). Our previous study has shown that PRG-N-01 does not affect Smad phosphorylation mediated by TβR1, unlike the TβR1 kinase inhibitor TEW7197.[19] Therefore, it suggests that PRG-N-01 could minimize side effects originating from inhibition of the TβR1 kinase activity, not like other inhibitors.

Intraperitoneal Administration of PRG-N-01 Demonstrates Therapeutic Effects in Schwannoma of NF2 Model Mouse

In our previous study, PRG-N-01 showed the inhibitory effect on tumor growth in an allograft model with mouse schwannoma cells. To validate the efficacy of the drug, it is crucial to verify whether it is effective in transgenic mouse models. Prior to conducting in vivo efficacy testing, we assessed the anti-proliferative effect of PRG-N-01 on tumor cells derived from NF2 mouse model. We obtained primary *Nf2*-deficient tumor cells by culturing cells isolated from tumor tissues of dissected NF2 mouse model for one month, resulting in 2 types of homogeneous cell populations (#149 & #184) (**Supplementary Figure 3A**). Compare to mouse fibroblast Nor-10 and HEI-193 cells lacking both isoforms 1 and 2,[27] these cells did not express

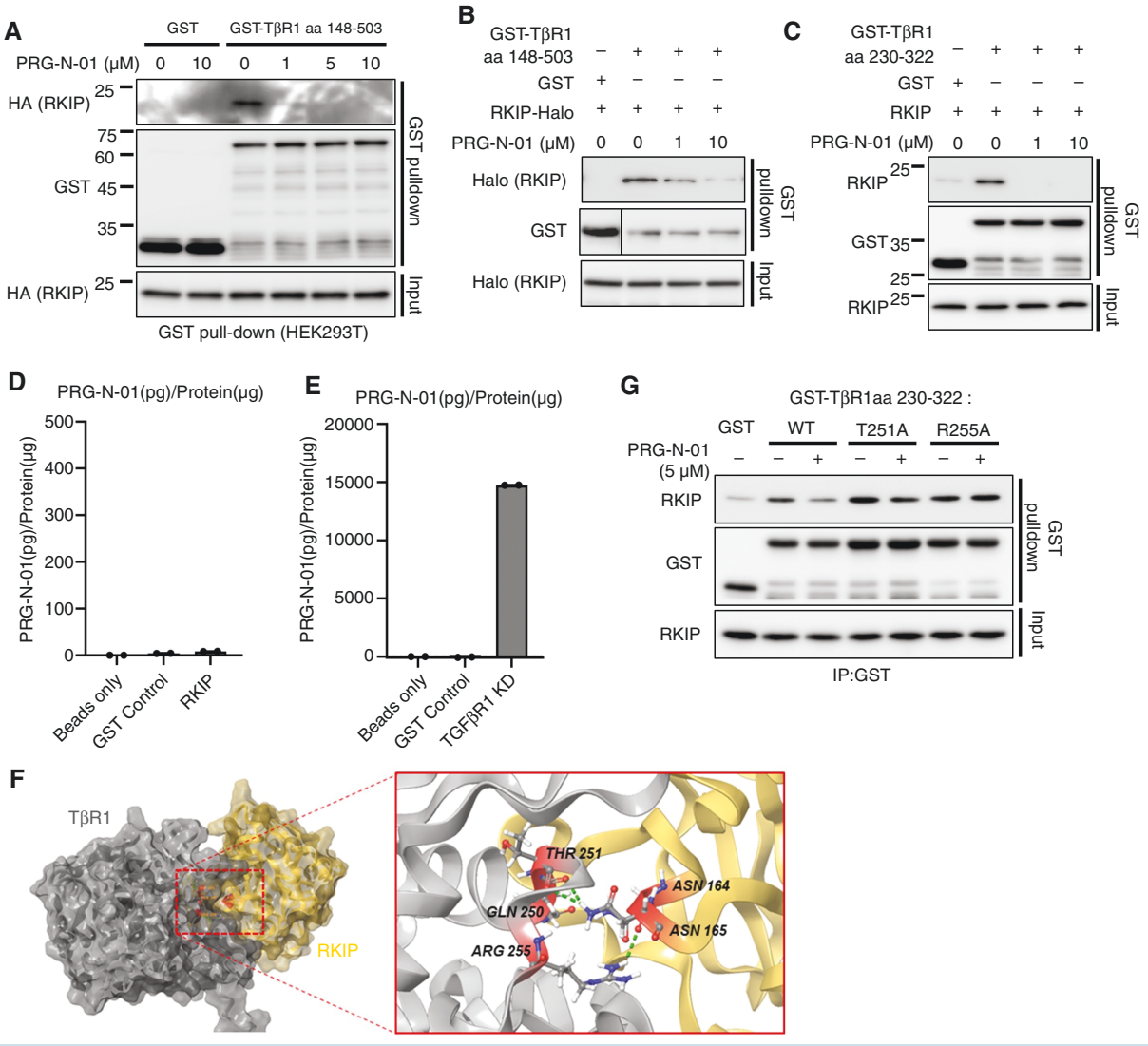

Figure 2. **Inhibition of the interaction between TβR1 aa 230-322 and RKIP by PRG-N-01. (A)** Bead-conjugated GST- TβR1 kinase domain (aa148-503) was co-incubated with RKIP-transfected HEK293T cell lysate and the indicated concentration of PRG-N-01 overnight and subjected to western blotting analysis. **(B)** In vitro TβR1 kinase domain (aa148-503)-RKIP binding assay with or without indicated concentration of PRG-N-01. **(C)** In vitro TβR1 (aa 230-322)-RKIP binding assay with or without indicated concentration of PRG-N-01. **(D and E)** The amounts of PRG-N-01 bound to GST-RKIP (D) or GST-TβR1 KD (E) were calculated by dividing the detected amount of PRG-N-01(pg) by each total protein quantity (ug). **(F)** Representation of 3D ribbon structure of plausible PRG-N-01 binding site. Residues 230-322 are highlighted and residues that are predicted to have hydrogen bonding interaction with RKIP are also highlighted. The position of the predicted PRG-N-01 binding site occupies a region closely related to these key residues, potentially blocking RKIP from binding. **(G)** In vitro binding of RKIP with GST-tagged TbR1 WT (aa 230-322) or various mutants in the presence of DMSO or PRG-N-01.

merlin. To evaluate the drug efficacy, we utilized #184 cells, which completely lack the merlin protein (**Supplementary Figure 3B**). Treatment with PRG-N-01 resulted in a dose-dependent reduction in the proliferation of #184 cells (Figure 3A**)**, while the expression of Schwann cell differentiation markers, GFAP was increased (Figure 3B). These findings demonstrate that PRG-N-01 has the potential to prevent *Nf2*-deficient tumor cell proliferation in the NF2 mouse model. Restoration of NF2 expression also reduced proliferation of #184 cells (**Supplementary Figure 3C and D**). The NF2 mouse model used in this study is a genetically engineered *Postin-Cre; Nf2*$^{flox/flox}$ mouse model.[28] These mice develop spinal, peripheral, and cranial nerve tumors that closely resemble human schwannomas by 10 months of age, with 100% penetrance.[29] To confirm the therapeutic effect of PRG-N-01 in this model mouse, PRG-N-01 was administered at the 9 months of age through intraperitoneal (i.p.) injection (Figure 3C). *Postin-Cre; Nf2*$^{flox/flox}$ mice exhibit spontaneous Schwann cell hypertrophy or schwannoma in the dorsal root ganglion (DRG) from 5 months of age, and all mice at 15 months of age possess significantly enlarged DRG.[29] Based on this information,

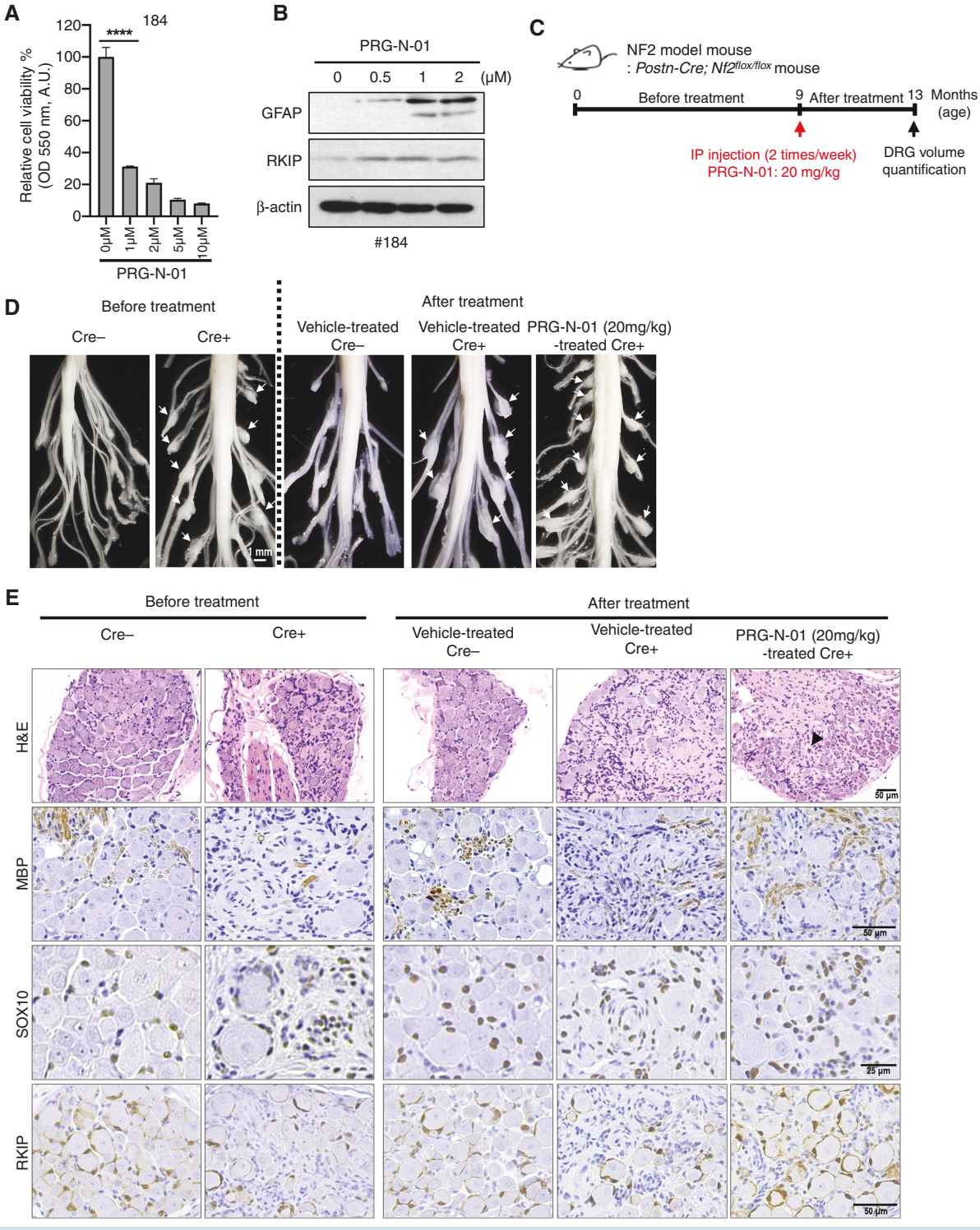

Figure 3. **Therapeutic effect of PRG-N-01 in NF2 model mouse.** (A) MTT assay of #184 cells treated with indicated concentration of PRG-N-01 for 3 days. Data are represented as mean ± SD. One-way ANOVA with Dunnett's multiple comparison test: ****$P < .0001$. (B) #184 cells were incubated with the indicated concentration of PRG-N-01 for 3 days. Protein lysates were analyzed by Western blotting with the specified antibodies. (C) Schematic of administration and tumor regression efficacy testing of PRG-N-01 in the NF2 mouse model. (D) Representative magnified images of the gross DRG from Cre- mice ($n = 2$, first from the left) and Cre+ mice ($n = 3$, second from the left) before PRG-N-01 administration, as well as from vehicle-treated Cre- mice ($n = 2$, third from the left) and Cre+ mice ($n = 3$, fourth from the left), and PRG-N-01 (20 mg/kg)-treated Cre+ mice ($n = 4$, fifth from the left) 5 months after administration. White arrows indicate the enlarged DRG. Scale bar = 1 mm. (E) Histological features of the representative H&E stain of the DRG of each group. Note the Schwann cell whorls formed in the enlarged ganglions of NF2 mouse models (first row, arrows). Representative images of immunostained DRG sections for MBP (second row), SOX10 (third row), and RKIP (fourth row) from each group before and after treatment with vehicle or PRG-N-01 (20 mg/kg).

we checked the occurrence of schwannoma in NF2 mouse model at 9 months of age and the volumes of DRG from dissected spinal cords were increased (**Figure 3D**). After 5 months of treatment, the vehicle-treated group showed a noticeable increase in DRG size, whereas the PRG-N-01-treated group did not exhibit a significant increase in overall tumor size (**Figure 3D and Supplementary Figure 4A**), particularly showing a marked reduction in the proportion of large tumors (> 0.8 mm) in lumbar regions (**Figure 3D and Supplementary Figure 4B**). To further investigate in vivo therapeutic effects of PRG-N-01, we evaluated the expression level of Schwann cell differentiation markers, including myelin basic protein (MBP), SRY-Box Transcription Factor 10 (SOX10)[30] and RKIP, in tumor tissue following PRG-N-01 administration (**Figure 3G**). Immunohistochemistry showed increased expression of MBP (**Supplementary Figure 4C**), SOX10 (**Supplementary Figure 4D**) and RKIP (**Supplementary Figure 4E**) in the DRG in the *Cre* + group administered with PRG-N-01. Schwannoma of the *Postin-Cre; Nf2*$^{flox/flox}$ exhibits similarities to NF2-SWN disease in humans, where histologically, Schwann cells proliferate and form whorls around the axon in DRG, eventually developing into a Schwannoma.[29] To investigate whether PRG-N-01 inhibits schwannoma formation in DRG, the number of whorl patterns formed by the proliferation of Schwann cells were counted. Compared to before treatment, the number of whorl patterns significantly increased in the 13-month Cre + vehicle-treated group, whereas the PRG-N-01-treated group showed a decrease (**Supplementary Figure 4F**). Analysis of the relationship between the number of RKIP-positive satellite cells and the number of Schwann cell whorls in the vehicle and PRG-N-01-treated group showed a negative correlation ($P < .05$) (**Supplementary Figure 4G**), suggesting that the reduced RKIP expression caused by *NF2* deficiency, could be a pivotal pathological mechanism driving NF2-related tumorigenesis. These results demonstrate that in vivo administration of PRG-N-01 may have therapeutic potential for NF2 syndrome by inhibiting tumorigenic growth and promoting differentiation of *NF2*-deficient Schwann cells.

PRG-N-01 Exhibits Preventive Effect Against Schwannoma in NF2 Mouse model via Oral Administration

Given that NF2-SWN manifests in adolescence and persists lifelong, assessing the preventive efficacy of PRG-N-01 via oral administration is essential. PRG-N-01 was administered beginning at the 11 weeks of age (**Figure 4A**). To evaluate the prevention potential of PRG-N-01, mice were orally administered 25 or 50 mg/kg of the drug mixed with their diet for 9 or 13 months. The control group received a diet mixed with vehicle (solvent only) under the same conditions (Figure 4A). PET/CT with 18F-FDG enables the detection of glycolytic activity and radiotracer accumulation in tumor areas,[31] which reflects the intensity of tumor glucose metabolism.[32] In this study, the decreased patterns of tumor location numbers and radioactivity uptake intensities in the mice, to which PRG-N-01 was orally administered for 9 months, were examined (**Figure 4B, C and Supplementary Figure 5A**). Noticeably, the strongest reduction of radiotracer accumulation was observed in the periorbital area of the PRG-N-01-treated group (Figure 4D). These findings suggest that PRG-N-01 may effectively suppress spontaneous multiple schwannoma formation in the NF2 mouse model. The DRG volume in *Cre* + PRG-N-01-treated group was significantly reduced by 49.4% compared to the vehicle-treated group (**Supplementary Figure 5B and C**) in both the thoracic (**Supplementary Figure 5D**) and lumbar regions (**Supplementary Figure 5E**). The number of whorl patterns was not observed at all in the untreated *Cre*- group, whereas it was significantly increased in the vehicle-treated *Cre*+ group (Figure 4E). However, in comparison to number of whorl patterns in the vehicle-treated group, their number in the PRG-N-01-treated Cre+ groups was significantly reduced by 55.9% and 54.9%. (**Supplementary Figure 5F**). These findings suggest that PRG-N-01 can effectively suppress *Nf2*-deficient Schwann cell proliferation in DRG. In DRG tissue, the expression level of Schwann cell differentiation markers, MBP and SOX10, was increased (Figure 4F, **Supplementary Figure 5G, H**). Furthermore, the number of RKIP-positive satellite cells wrapping around axons was decreased in the Cre+ group compared to the control group (**Supplementary Figure 5I**) and the reduction was rescued by the administration of PRG-N-01 (**Supplementary Figure 5J**). The number of RKIP-positive satellite cells and Schwann cell whorls in the vehicle and PRG-N-01-treated group showed a negative correlation ($p < 0.05$) (**Supplementary Figure 5K**). These results indicate that administering PRG-N-01 at an early stage demonstrates a disease-preventive effect for NF2-SWN.

Gene Expression Profile of Dorsal Root Ganglia Schwannoma of PRG-N-01-treated NF2 Mouse Model

To explore the effect of PRG-N-01 on gene expression in the mouse model, we conduct RNA sequencing in the dorsal root ganglia (DRG) of vehicle-treated (G3) and PRG-N-01-treated NF2 mouse model (G4). Our analysis revealed a distinct group of 180 differentially expressed genes (DEGs) in the DRGs, with 157 genes being down-regulated and 23 genes up-regulated upon PRG-N-01 treatment. These DEGs are well divided into G3 and G4 groups (**Supplementary Figure 6A and B**). Gene set enrichment analysis (GSEA) indicated 23 statistically significant Hallmark gene sets. In the PRG-N-01-treated group, mitotic spindle gene sets were depleted; in contrast, oxidative phosphorylation (OXPHOS) and fatty acid metabolism gene sets were enriched (**Supplementary Figure 6C**). This suggests that PRG-N-01 treatment inhibits tumor growth drivers in the DRG of the NF2 mouse model while promoting gene sets associated with oxidative phosphorylation and lipid metabolism. Importantly, the enhancement of OXPHOS in PRG-N-01 treated groups signifies a reversal of the typical metabolic reprogramming observed in various cancer cells, where glycolysis is enhanced and OXPHOS capacity is diminished.[33] Upregulation of fatty acid gene sets suggests that PRG-N-01 promotes Schwann cell differentiation by facilitating the metabolic processes essential for myelin production.[34] Notably, the leading-edge genes in the oxidative phosphorylation and the fatty acid metabolism gene sets were significantly upregulated, while those in the mitotic spindle assembly sets were significantly downregulated (**Supplementary**

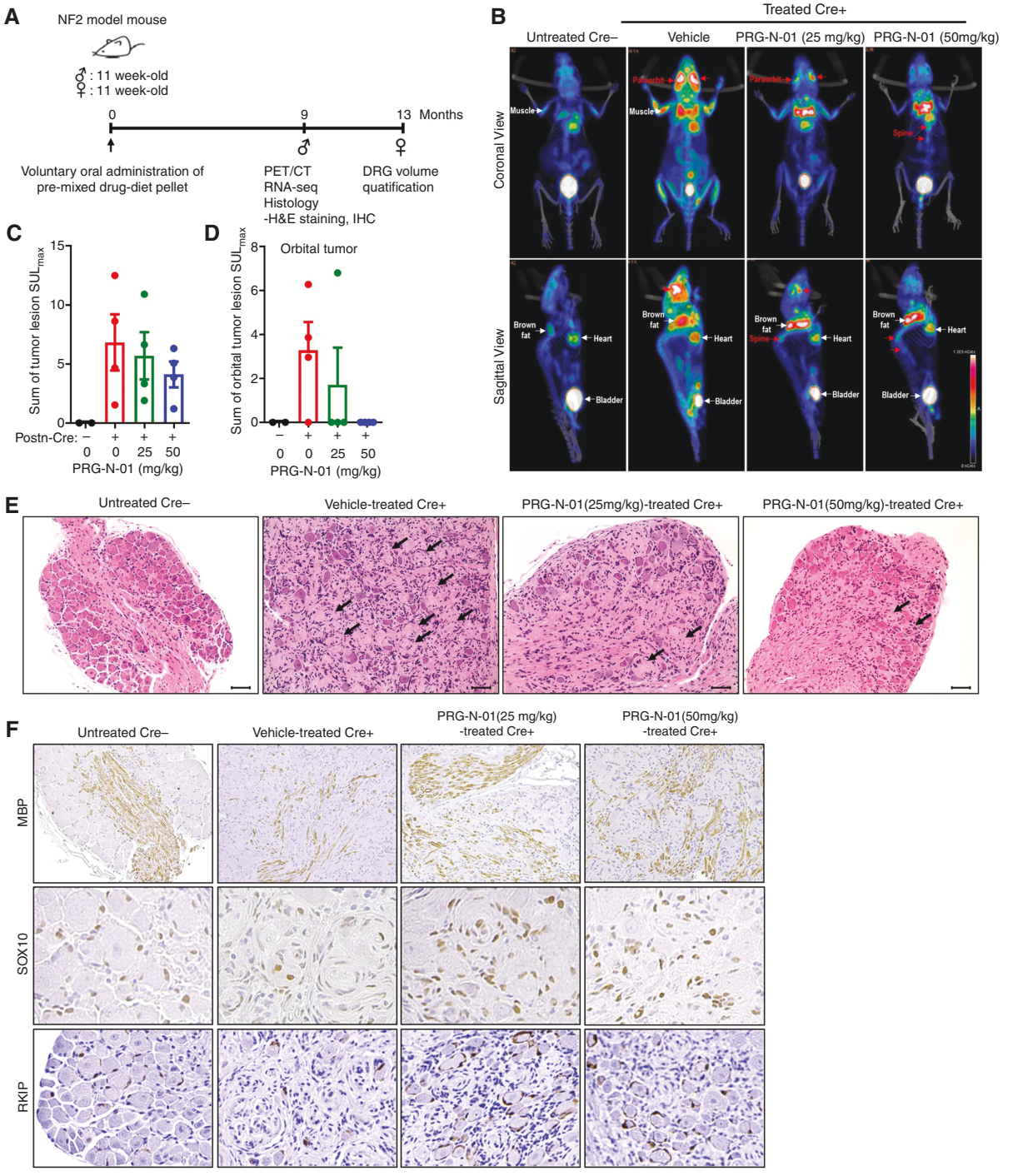

Figure 4. **Prevention effect of PRG-N-01 in NF2 model mouse via early oral administration.** (A) Schematics of administration and anti-tumor efficacy testing of PRG-N-01 in NF2 mouse model. (B) Whole-body micro-PET/CT images of NF2 mouse model post-treated 9 months with vehicle or PRG-N-01. Red arrow indicates the tumor lesions, and physiologic tracer uptake in muscle, heart, brown fat, and bladder is marked (white arrow). Untreated Cre-, $n = 2$ mice; Vehicle-treated Cre+, $n = 4$ mice; PRG-N-01 (25 mg/kg)-treated Cre+, $n = 4$ mice; PRG-N-01 (50 mg/kg)-treated Cre+, $n = 4$ mice. (C-D) Maximum standardized uptake value (SULmax) in the whole body (C) and orbital region (D) after fasting and glucose loading. Untreated Cre-, $n = 2$ mice; Vehicle-treated Cre+, $n = 4$ mice; PRG-N-01 (25 mg/kg)-treated Cre+, $n = 4$ mice; PRG-N-01 (50 mg/kg)-treated Cre+, $n = 4$ mice. (E) Histological features of the representative hematoxylin and eosin (H&E) stain of the dorsal root ganglion of each group. Note the Schwann cell whorls formed in the enlarged ganglions of NF2 mouse models (arrows). The whorls of Schwann cell proliferation observed upper right are characteristic of schwannoma histology. (F) Representative images of immunostained sections of the DRG of *Nf2*-deficient mice treated with vehicle or PRG-N-01 (25 mg/kg) or PRG-N-01 (50 mg/kg) for myelin basic protein (MBP, upper), SOX10 (middle) and RKIP (lower).

Figure 6D and E). RT-qPCR validation revealed that PRG-N-01 induced an increase in oxidative phosphorylation-related genes, such as *NDUFB8* and *NDUFA4* and lipid metabolism–related genes, such as *S100A10* and *EPHX1* in HEI-193 cells (**Supplementary Figure 6F-I**). These findings strongly support our in vivo results, suggesting that PRG-N-01 not only suppresses Schwannoma formation but also promotes the differentiation of tumor cells into Schwann cells in the NF2 mice model (**Figures 3** and **4**).

Comparative Study of PRG-N-01, Brigatinib, and Selumetinib for the Treatment of *Nf2*-deficient Schwannoma Cells

For the treatment of NF2-SWN, several targeted therapies used in various cancers are being applied and clinical phase 2 trials are currently underway. One trial involves the use of Brigatinib (NCT04374305), a small molecule inhibitor that targets FAK1 and EphA2 in the NF2-associated signaling cascade,[35] while the other involves Selumetinib (NCT03095248), a MEK1 inhibitor that targets the Ras/ERK signaling cascade.[36] We compared the in vitro antiproliferative effects of PRG-N-01 with that of Brigatinib and Selumetinib in *NF2*-deficient tumor cells. Both PRG-N-01 and Brigatinib dose-dependently reduced the proliferation of HEI-193 cells, whereas Selumetinib did not exhibit any effect (Figure 5A). Furthermore, PRG-N-01 showed the most significant growth inhibition in primary mouse *Nf2*-deficient tumor cells (Figure 5B). However, Brigatinib showed toxicity in human normal fibroblasts even at low concentration, while PRG-N-01 did not exhibit any significant cytotoxic effect even at high concentrations (**Figure 5C**). Brigatinib induced cytochrome c release from mitochondria[37] (Figure 5D) and activated caspase-3,[38] and inactivated PARP[39] in normal fibroblast, suggesting apoptosis (Figure 5E). Caspase-3 activation and PARP inactivation were also observed in HEI-193 cells treated with Brigatinib (Figure 5F). While, treatment with PRG-N-01, regardless of the concentration used, decreased the expression of stem cell factor SOX2 but increased the expression of a Schwann cell differentiation marker SOX10, MBP,[28] and cell cycle negative regulators p21[40] and p27[41] in Hei-193 cells (**Figure 5G and Supplementary Figure 7A-F**). Brigatinib decreased the expression of all these markers. In contrast to Brigatinib, treatment with PRG-N-01 did not affect the total cell count, but the number of S100B-positive cells, representing Schwann cell, decreased in NF2-SWN patients derived to primary human vestibular schwannoma (VS) cells (**Supplementary Figure 8A-C**). Additionally, PRG-N-01 downregulated SOX2, a stem cell factor, but upregulated Schwann cell differentiation markers SOX10, MPZ, and GFAP (**Supplementary Figure 8D**). These findings demonstrate the selective anti-cell growth effect of PRG-N-01 on human primary VS cells, supporting its potential as a therapeutic agent targeting *NF2*-deficient schwannoma.

Preclinical Profiling of PRG-N-01

To determine whether PRG-N-01 could successfully proceed to clinical trials, we conducted preclinical research. PRG-N-01 was soluble up to 100 μM in 0.3% DMSO in extracellular solution (ECS) with a pH of 6.9, and stable in plasma from CD-1 mice, SD rats, beagle dogs, cynomolgus monkeys, and humans after 120 min (**Supplementary Table 1**). It showed high permeability in Caco-2 cells without being a significant BCRP substrate and demonstrated moderate permeability across MDR1-MDCK II cells, indicating it is not a strong P-glycoprotein substrate (**Supplementary Table 2**). PRG-N-01 underwent high metabolism in CD-1 mouse and beagle dog hepatocytes, moderate metabolism in SD rat, cynomolgus monkey, and human hepatocytes (**Supplementary Table 1**), and showed moderate to slow metabolism in liver microsomes across these species (**Supplementary Table 1**). Pharmacokinetic studies revealed low clearance rates (29.3 to 66 mL/min/kg CL), long elimination half-lives (1.03 to 2.03 h), and low to moderate distribution volumes (1.3 to 5 liter/kg) post-intravenous injection (**Figure 6A–D**). Oral administration led to moderate to high bioavailability (52.3% in mice, 54.9% in rats, 68.8% in dogs) with peak blood concentration (T_{max}) between 0.67 and 24.7 h (**Figure 6A–D**). Dose-related increases in maximum blood concentration and exposure were noted (Figure 6D), indicating good oral availability and pharmacokinetic properties of PRG-N-01 in preclinical species.

To establish the safety of PRG-N-01, particularly for NF2-SWN patients who may require combination therapy and have additional health complications, a comprehensive panel of in vitro safety assays was performed. PRG-N-01 was not found to be a substrate for the transporters OATP1B1, OATP1B3, OAT1, OAT3, OCT2, MATE1, and MATE2-K under tested conditions. However, it inhibited OCT2, MATE1, and MATE2-K with IC50 values of 0.663, 1.30, and 1.25 μM, respectively, indicating potential drug-drug interaction (DDI) risks (**Supplementary Table 2**). Importantly, PRG-N-01 did not inhibit any major cytochrome (CYP) enzymes (CYP 1A2/2B6/2C8/2C9/2C19/2D6/3A), although CYP2C8 was identified as a major metabolic enzyme for metabolite M5 formation, with CYP3A also potentially involved (**Supplementary Tables 2, 3, and 6**). Further in-depth studies are currently underway to assess DDI risks more comprehensively.

In evaluating the effects of PRG-N-01 on human ether-à-go-go related gene (hERG) potassium channels via automated patch clamp in HEK293 cells, it exhibited low cardiotoxicity with an IC50 of 15.66 μM (**Supplementary Table 4**). Additionally, PRG-N-01 showed low genetic toxicity risk in mini Ames and micronucleus assays, indicating minimal mutagenicity and chromosomal damage (**Supplementary Table 5**). Testing against a panel of receptors, channels, and enzymes, PRG-N-01 significantly affected Alpha2A by 60.94% at 10 μM, with negligible effects on 33 other targets (**Supplementary Table 6**).

In assessing the safety of PRG-N-01, single-dose toxicity tests showed maximum tolerated doses of 300 mg/kg in rats and 1000 mg/kg in dogs (**Supplementary Table 5**). Follow-up studies, including 2 and 4-week repeated oral toxicity tests, aimed to evaluate long-term effects and established the no-observed-adverse-effect level (NOAEL) at 25 mg/kg in rats and 80 mg/kg in dogs. These results indicate a promising safety profile of PRG-N-01 for clinical development (**Supplementary Table 5**).

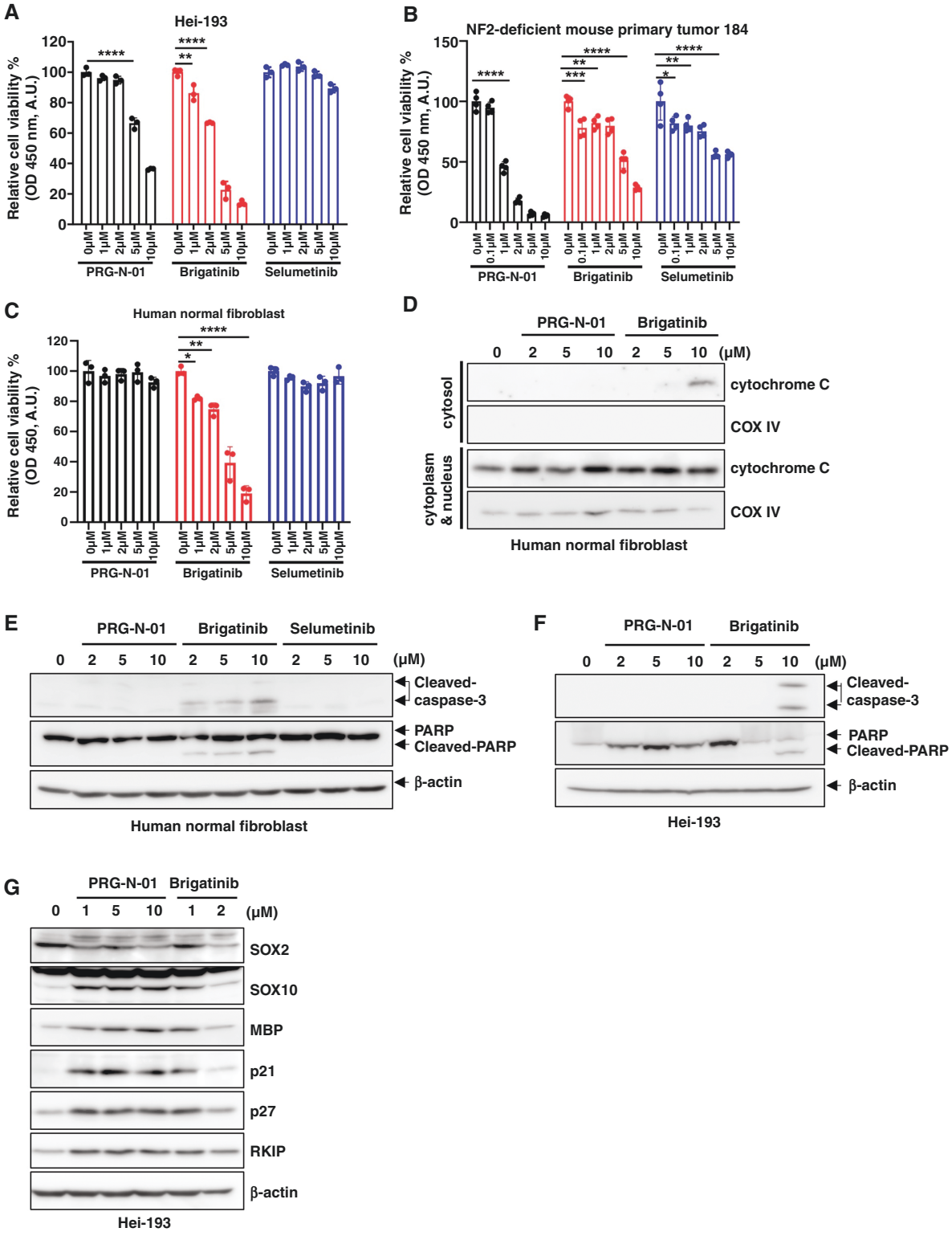

Figure 5. PRG-N-01 demonstrates the competitive advantage over other drugs. (A-C) HEI-193 cells (A) or *Nf2*-deficient mouse primary tumor (#184) (B) or normal human fibroblasts (C) were incubated with the indicated concentration of chemicals for 3 days, and cell viability was measured using WST-8 assay. The results in A, B, and C are representative of 3 independent experiments, and bar graph data show the mean ± SD. One-way ANOVA with Dunnett's multiple comparison test: $^{*}P < .05$, $^{**}P < .01$, $^{***}P < .01$, and $^{****}P < .0001$. (D) Normal human fibroblasts were incubated with the indicated concentration of chemicals for 1 day. For the detection of cytochrome c release, cytosolic fractions were prepared as described in Materials and Methods. Cytochrome c oxidase subunit IV (COX IV) was used as a mitochondrial marker. (E and F) Western blot analysis of cleaved-caspase-3 and cleaved-PARP expression after treatment with the indicated concentration of chemical for 24 hr in normal human fibroblasts (E) or HEI-193 cells (F). (G) To compare differentiation into Schwann cells, HEI-193 cells were incubated with the indicated concentration of chemicals for 7 days and subjected to western blotting analysis. The results in D, E, F, and G are representative immunoblot of 3 independent experiments.

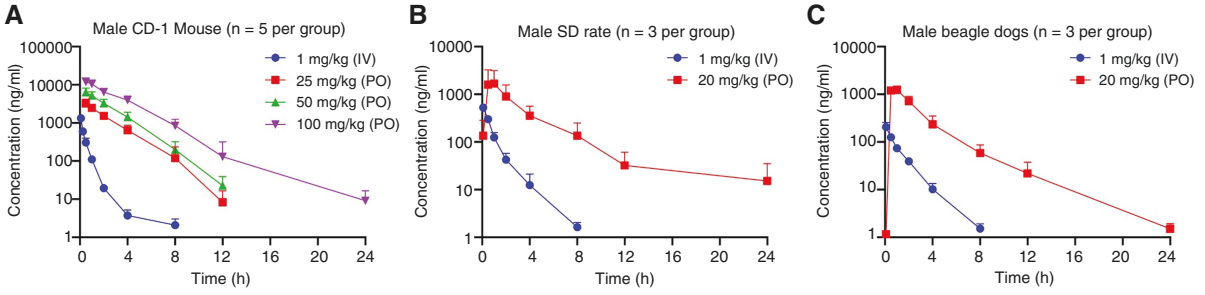

D

Species	Dose (mg/kg)		Vdss (L/kg)	CL (mL/min/kg)	Cmax (ng/mL)	Tmax (h)	AUC0-last (ng/mL*h)	BA (%)
	Pharmacokinetics Parameter							
Mouse	1	IV	1.30	29.3	—	—	575	—
	25	PO	—	—	3266	0.6	7593	52.3
	50	PO	—	—	6355	0.5	15779	54.3
	100	PO	—	—	11922	0.5	36945	63.5
Rat	1	IV	2	37	—	—	457	—
	20	PO	—	—	1746	0.67	4942	54.9
Dog	1	IV	5	66	—	—	246	—
	20	PO	—	—	1340	0.67	3433	68.8

E

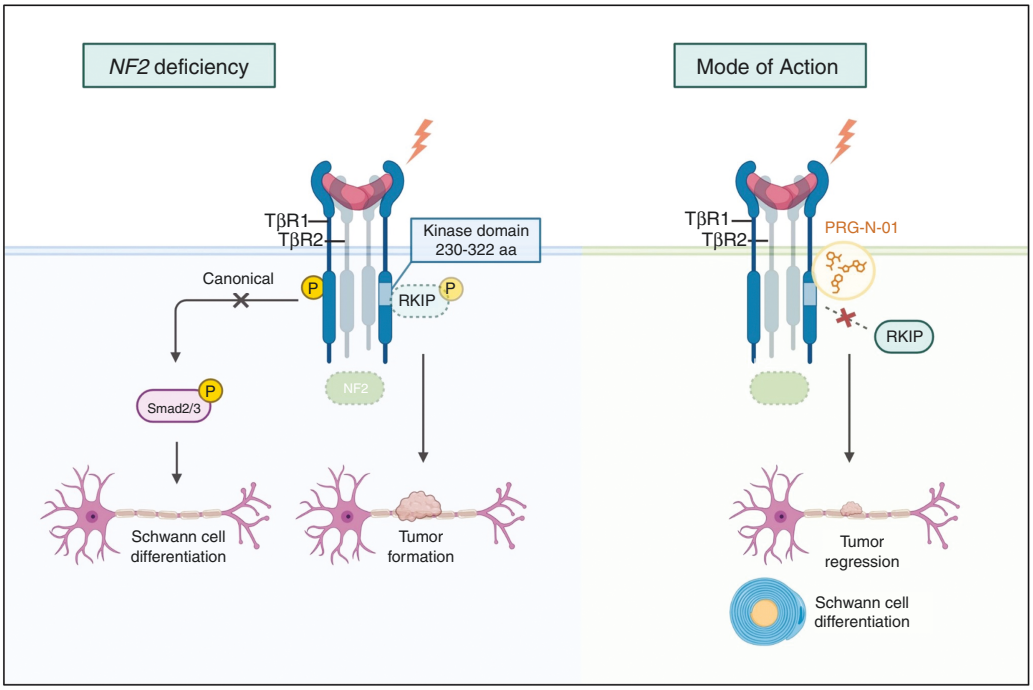

Figure 6. **The pharmacokinetic profile of PRG-N-01.** Mean plasma concentration of PRG-N-01 after IV bolous and PO dosing in mice, rats, and dogs. (A) Male CD-1 mouse ($n = 5$ per group) were dosed intravenously (IV) with 1 mg/kg or orally (PO) with PRG-N-01 at 25 mg/kg, 50 mg/kg, 100 mg/kg. (B) Male SD rats ($n = 3$ per group) were dosed intravenously (IV) with 1 mg/kg or orally (PO) with PRG-N-01 at 20 mg/kg. (C) Beagle dogs ($n = 3$ per group) were dosed intravenously with 1 mg/kg or orally with PRG-N-1 at 20 mg/kg. Whole-blood samples were taken at various time points up to 24 h, and PRG-N-01 concentration was measured using liquid chromatography–mass spectrometry. (D) Oral and intravenous pharmacokinetics in preclinical species. Animals were dosed once daily. Mouse pharmacokinetic (PK) samples were taken from animals during the in vivo efficacy study. Cmax, maximum blood concentration; T_{max}, time of peak blood concentration; AUC, area under the curve ($t = 0$ to infinite); Vdss, volume of distribution at steady state; CL, clearance from blood; Elim T1/2, elimination half-life. (E) Potential mechanisms by which PRG-N-01 treatment suppressed the NF2 syndrome-related tumor formation. Under healthy conditions, physical stress or contact did not activate TβR1 due to the inhibitory effect of TβR2. However, under *NF2*-deficient conditions, extracellular physical stresses may activate TβR1 kinase and reduce RKIP expression. Thus, inhibition of TβR1-RKIP interaction is a potential therapeutic strategy for NF2 syndrome. PRG-N-01 binds to the TβR1 kinase domain and inhibits the direct interaction between TβR1 and RKIP without affecting canonical TGF-β signaling. PRG-N-01 treatment effectively inhibits schwannoma formation in NF2 mouse model.

Discussion

The majority of NF2-SWN patients harbor *NF2* gene mutations, resulting in an imbalance of TGF-β receptors that promotes TβR1-mediated phosphorylation and degradation of RKIP.[18] In a previous study, we developed a novel NF2-SWN therapeutic candidate, PRG-N-01 (new code name of Nf18001), which inhibits TβR1-mediated RKIP degradation without disrupting canonical TGF-β signaling.[19] Understanding more detailed molecular mechanisms of PRG-N-01 and validating efficacy in model mice and obtaining preclinical data is essential for developing clinical treatment for patients with NF2-SWN. PRG-N-01 effectively disrupts the binding between TβR1 and RKIP by targeting the amino acids 230-322 of TβR1, which are crucial for RKIP binding (Figures 1C, 1D and 2C). The in vitro binding assay further confirms these findings by showing that PRG-N-01 readily binds to the TβR1 kinase domain but not to RKIP (Figure 2D and E). Based on the inhibitory effect of PRG-N-01 on tumor growth in an allograft model with mouse schwannoma cells, we assessed the efficacy of PRG-N-01 using the NF2 mouse model (*Postn-Cre*; *Nf2*$^{f/f}$) in this study. The therapeutic effect in the mouse model was confirmed by administering PRG-N-01 via i.p. injection after tumor formation (**Figure 3**). The volume of DRG and the number of whorl patterns reflecting the occurrence of Schwann cell hypertrophy or schwannoma, was decreased in the PRG-N-01-treated group. Besides, the expression of schwann cell differentiation markers and RKIP was increased (Figure 3 **and Supplementary Figure 4**). PRG-N-01 also has an NF2-SWN prevention effect via early oral administration by demonstrating inhibition of schwannomagenesis and inducing tumor cell differentiation in the *Nf2*-deficient mice model (Figure 3). Transcriptome analysis demonstrates the tumor growth inhibitory effect and the normal metabolism and cell differentiation promoting effect by PRG-N-01 (**Supplementary Figure 6**), strongly supporting our in vivo results (Figures 2 and 3). The in vitro antitumor efficacy of PRG-N-01, Brigatinib, and Selumetinib in *NF2*-deficient tumor cells was compared (Figure 5A and B). Notably, PRG-N-01 showed no significant cytotoxicity against human normal fibroblasts in contrast to Brigatinib (Figure 5C and F). Stem cell factor SOX2 was decreased, and Schwann cell differentiation marker and cell cycle negative regulators were increased by PRG-N-01 treatment (Figure 5G).

Furthermore, the pharmacokinetics (Figure 6), metabolic stability (**Supplementary Table 1**) and safety profile (**Supplementary Tables 4** and **5**) of PRG-N-01 were investigated both in vitro and in vivo, demonstrating its druggability is promising. NF2-SWN manifests during adolescence and has a wide range of severity, necessitating long-term treatment, which makes the development of orally administered medications essential. Our preclinical data indicate that PRG-N-01 has good metabolic stability, favorable pharmacokinetics upon oral administration, and a bioavailability (BA) exceeding 50% in all cases. Therefore, the development of an oral formulation for PRG-N-01 appears to be highly promising. Based on repeated oral toxicity tests and following cautious dosing recommendations for the first administration in humans, the starting dose was set at 25 mg, and it will be increased to a maximum of 50 mg through an accelerated titration design. Phase 1/2a study to find dose and to evaluate the efficacy and safety of PRG-N-01 in patients with NF2-SWN are currently underway in South Korea.

The dysregulation of the TGF-β signaling pathway is believed to play a pivotal role in the development of colon cancer, affecting various TGF-β-mediated processes like growth inhibition, apoptosis, differentiation, and other TGF-β-controlled functions.[42,43] The most prevalent mechanism contributing to TGF-β signaling dysregulation in colon cancers involves the mutational inactivation of TβR2. This inactivation of TβR2 within colon cancer cells contributes to the malignant characteristics of the disease through multiple pathways, including Wnt-β-catenin, Hippo, and MAPK.[44] Previously, our group showed that reduction of TβR2 expression leads to the non-canonical activation of TβR1, thereby promoting cell proliferation through the activation of MAPK and Snail.[18,19] In this study, we provide evidence that PRG-N-01 could bind TβR1 kinase domain but not affect its kinase activity, thereby suppressing schwannoma formation in an NF2-SWN mouse model. Therefore, it is worth investigating whether the binding capacity of PRG-N-01 to TβR1 could be linked to pathology of the TβR2-inactivated colon cancer.

In conclusion, our study provides preliminary evidence that PRG-N-01, a first-in-class drug, may represent a promising treatment option for NF2-SWN. PRG-N-01 exhibits several unique features that differentiate it from other NF2-SWN therapies currently under investigation. We look forward to the upcoming clinical trials for healthy volunteers and patients with NF2-SWN-related tumors. While additional studies are needed to confirm its safety and efficacy in humans, the development of PRG-N-01 as a targeted therapy for NF2-SWN possess significant potential for improving the lives of NF2-SWN patients.

Supplementary material

Supplementary material is available online at *Neuro-Oncology* (https://academic.oup.com/neuro-oncology).

Keywords

NF2-related schwannomatosis (NF2-SWN) | Merlin | TGFβR1 | RKIP | new drug candidate

Acknowledgments

We thank Dr. In Seok Moon at the Department of Otorhinolaryngology, Yonsei University College of Medicine, for providing vestibular schwannoma tissue of the NF2-SWN patient.

Conflict of interest statement

Yeon-Ho Chung, Bae-Hoon Kim, Yeongseon Ji, Tae-Gyun Woo, Songyoung Baek, Eunbyeol Shin, Yi Jin Song, Yuju Kim, Jin Han, and Bum-Joon Park are employees of PRG S&T Co., Ltd.

Funding

This work was supported by National Research Foundation of Korea (NRF) grants funded by the Korean government (MSIT) (RS-2024-00399681, RS-2024-00339289 and RS-2024-00442484).

Authorship Statement

BJP, BHK, and YHC conceptualized the study, designed the study methodology, and supervised the study. SYP, YHC, BHK, ML, JL, HRK, and JC wrote the original draft of the manuscript. ML and JC conducted the RNA-seq and data analysis. JL and HRK conducted prediction of protein complex and molecular docking. YHC, JYS, SP, TGW, SB, ES, YIS, YJH, YK and HJ performed the experiment. SYP and MK were responsible for the administration of the preclinical study.

Data Availability

The data generated in this study are available within the article and its supplementary data files. All other data that support the findings of this study are available from the corresponding author upon reasonable request.

Affiliations

Department of Molecular Biology, College of Natural Science, Pusan National University, Busan, Republic of Korea (S.P., Y.J.H., B.-J.P.); Rare Disease R&D Center, PRG S&T Co., Ltd, Busan, Republic of Korea (Y.-H.C., Y.J., Y.J.S., T.-G.W., E.S., S.B., Y.K., M.K., J.H., B.-H.K., B.-J.P.); Department of Biomedical Sciences, Korea University College of Medicine, Seoul, Republic of Korea (M.L., J.L., H.-R.K., J.C.); Brain Korea 21 Plus Project for Biomedical Science, Korea University College of Medicine, Seoul, Republic of Korea (J.L.)

References

1. Asthagiri AR, Parry DM, Butman JA, et al. Neurofibromatosis type 2. *Lancet.* 2009;373(9679):1974–1986.
2. Merker VL, Esparza S, Smith MJ, Stemmer-Rachamimov A, Plotkin SR. Clinical features of schwannomatosis: a retrospective analysis of 87 patients. *Oncologist.* 2012;17(10):1317–1322.
3. Ammoun S, Hanemann CO. Emerging therapeutic targets in schwannomas and other merlin-deficient tumors. *Nat Rev Neurol.* 2011;7(7):392–399.
4. Mathieu D, Kondziolka D, Flickinger JC, et al. Stereotactic radiosurgery for vestibular schwannomas in patients with neurofibromatosis type 2: an analysis of tumor control, complications, and hearing preservation rates. *Neurosurgery.* 2007;60(3):460–8; discussion 468.
5. Plotkin SR, Stemmer-Rachamimov AO, Barker FG, 2nd, et al. Hearing improvement after bevacizumab in patients with neurofibromatosis type 2. *N Engl J Med.* 2009;361(4):358–367.
6. Slusarz KM, Merker VL, Muzikansky A, Francis SA, Plotkin SR. Long-term toxicity of bevacizumab therapy in neurofibromatosis 2 patients. *Cancer Chemother Pharmacol.* 2014;73(6):1197–1204.
7. Petrilli AM, Fernández-Valle C. Role of Merlin/NF2 inactivation in tumor biology. *Oncogene.* 2016;35(5):537–548.
8. Hamaratoglu F, Willecke M, Kango-Singh M, et al. The tumour-suppressor genes NF2/Merlin and expanded act through hippo signalling to regulate cell proliferation and apoptosis. *Nat Cell Biol.* 2006;8(1):27–36.
9. Cui Y, Groth S, Troutman S, et al. The NF2 tumor suppressor merlin interacts with Ras and RasGAP, which may modulate Ras signaling. *Oncogene.* 2019;38(36):6370–6381.
10. Lallemand D, Curto M, Saotome I, Giovannini M, McClatchey AI. NF2 deficiency promotes tumorigenesis and metastasis by destabilizing adherens junctions. *Genes Dev.* 2003;17(9):1090–1100.
11. Yeung K, Seitz T, Li S, et al. Suppression of Raf-1 kinase activity and MAP kinase signalling by RKIP. *Nature.* 1999;401(6749):173–177.
12. Maresch J, Birner P, Zakharinov M, et al. Additive effect on survival of Raf kinase inhibitor protein and signal transducer and activator of transcription 3 in high-grade glioma. *Cancer.* 2011;117(11):2499–2504.
13. Lin X, Bai F, Nie J, et al. Didymin alleviates hepatic fibrosis through inhibiting ERK and PI3K/Akt pathways via regulation of Raf kinase inhibitor protein. *Cell Physiol Biochem.* 2016;40(6):1422–1432.
14. Escara-Wilke J, Yeung K, Keller ET. Raf kinase inhibitor protein (RKIP) in cancer. *Cancer Metastasis Rev.* 2012;31(3-4):615–620.
15. Kim HS, Kim GY, Lim SJ, Kim YW. Raf-1 kinase inhibitory protein expression in thyroid carcinomas. *Endocr Pathol.* 2010;21(4):253–257.
16. Hagan S, Al-Mulla F, Mallon E, et al. Reduction of Raf-1 kinase inhibitor protein expression correlates with breast cancer metastasis. *Clin Cancer Res.* 2005;11(20):7392–7397.
17. Cho JH, Lee SJ, Oh AY, et al. NF2 blocks snail-mediated p53 suppression in mesothelioma. *Oncotarget.* 2015;6(12):10073–10085.
18. Cho JH, Oh AY, Park S, et al. Loss of NF2 induces TGFβ receptor 1-mediated noncanonical and oncogenic TGFβ signaling: implication of the therapeutic effect of TGFβ receptor 1 inhibitor on NF2 syndrome. *Mol Cancer Ther.* 2018;17(11):2271–2284.
19. Cho JH, Park S, Kim S, et al. RKIP induction promotes tumor differentiation via SOX2 degradation in NF2-deficient conditions. *Mol Cancer Res.* 2022;20(3):412–424.
20. Zinzalla G, Thurston DE. Targeting protein-protein interactions for therapeutic intervention: a challenge for the future. *Future Med Chem.* 2009;1(1):65–93.
21. Ventura F, Liu F, Doody J, Massagué J. Interaction of transforming growth factor-beta receptor I with farnesyl-protein transferase-alpha in yeast and mammalian cells. *J Biol Chem.* 1996;271(24):13931–13934.
22. Wrana JL, Attisano L, Wieser R, Ventura F, Massagué J. Mechanism of activation of the TGF-beta receptor. *Nature.* 1994;370(6488):341–347.
23. Luo K, Lodish HF. Signaling by chimeric erythropoietin-TGF-beta receptors: homodimerization of the cytoplasmic domain of the type I TGF-beta receptor and heterodimerization with the type II receptor are both required for intracellular signal transduction. *EMBO J.* 1996;15(17):4485–4496.
24. Macías-Silva M, Abdollah S, Hoodless PA, et al. MADR2 is a substrate of the TGFbeta receptor and its phosphorylation is required for nuclear accumulation and signaling. *Cell.* 1996;87(7):1215–1224.

25. Zhang Y, Feng X, We R, Derynck R. Receptor-associated Mad homologues synergize as effectors of the TGF-beta response. *Nature*. 1996;383(6596):168–172.
26. Yeung K, Janosch P, McFerran B, et al. Mechanism of suppression of the Raf/MEK/extracellular signal-regulated kinase pathway by the raf kinase inhibitor protein. *Mol Cell Biol*. 2000;20(9):3079–3085.
27. Lepont P, Stickney JT, Foster LA, et al. Point mutation in the NF2 gene of HEI-193 human schwannoma cells results in the expression of a merlin isoform with attenuated growth suppressive activity. *Mutat Res*. 2008;637(1-2):142–151.
28. Lindsley A, Snider P, Zhou H, et al. Identification and characterization of a novel Schwann and outflow tract endocardial cushion lineage-restricted periostin enhancer. *Dev Biol*. 2007;307(2):340–355.
29. Gehlhausen JR, Park SJ, Hickox AE, et al. A murine model of neurofibromatosis type 2 that accurately phenocopies human schwannoma formation. *Hum Mol Genet*. 2015;24(1):1–8.
30. Liu Z, Jin YQ, Chen L, et al. Specific marker expression and cell state of Schwann cells during culture in vitro. *PLoS One*. 2015;10(4):e0123278.
31. Fletcher JW, Djulbegovic B, Soares HP, et al. Recommendations on the use of 18F-FDG PET in oncology. *J Nucl Med*. 2008;49(3):480–508.
32. Kim JW, Dang CV. Cancer's molecular sweet tooth and the Warburg effect. *Cancer Res*. 2006;66(18):8927–8930.
33. Zheng J. Energy metabolism of cancer: glycolysis versus oxidative phosphorylation (Review). *Oncol Lett*. 2012;4(6):1151–1157.
34. Montani L, Pereira JA, Norrmén C, et al. De novo fatty acid synthesis by Schwann cells is essential for peripheral nervous system myelination. *J Cell Biol*. 2018;217(4):1353–1368.
35. Chang L-S, Dasgupta P, Oblinger JL, et al. Brigatinib causes tumor shrinkage in both NF2-deficient meningioma and schwannoma through inhibition of multiple tyrosine kinases but not ALK. *PLOS One*. 2021;16(7):e0252048.
36. Fuse MA, Dinh CT, Vitte J, et al. Preclinical assessment of MEK1/2 inhibitors for neurofibromatosis type 2–associated schwannomas reveals differences in efficacy and drug resistance development. *Neuro-Oncology*. 2019;21(4):486–497.
37. Liu X, Kim CN, Yang J, Jemmerson R, Wang X. Induction of apoptotic program in cell-free extracts: requirement for dATP and cytochrome c. *Cell*. 2004;86(1):147–157.
38. Nicholson DW, Ali A, Thornberry NA, et al. Identification and inhibition of the ICE/CED-3 protease necessary for mammalian apoptosis. *Nature*. 2003;376(6535):37–43.
39. Kaufmann SH, Desnoyers S, Ottaviano Y, et al. Specific proteolytic cleavage of poly(ADP-ribose) polymerase: an early marker of chemotherapy-induced apoptosis. *Cancer Res*. 1993;53(17):3976–3985.
40. Xiong Y, Hannon GJ, Zhang H, et al. p21 is a universal inhibitor of cyclin kinases. *Nature*. 2003;366(6456):701–704.
41. Ji P, Jiang H, Rekhtman K, et al. An Rb-Skp2-p27 pathway mediates acute cell cycle inhibition by Rb and Is retained in a partial-penetrance Rb mutant. *Molecular Cell*. 2004;16(1):47–58.
42. Grady WM, Myeroff LL, Swinler SE, et al. Mutational inactivation of transforming growth factor beta receptor type II in microsatellite stable colon cancers. *Cancer Res*. 1999;59(2):320–324.
43. Markowitz SD, Roberts AB. Tumor suppressor activity of the TGF-beta pathway in human cancers. *Cytokine Growth Factor Rev*. 1996;7(1):93–102.
44. Morris SM, Davison J, Carter KT, et al. Transposon mutagenesis identifies candidate genes that cooperate with loss of transforming growth factor-beta signaling in mouse intestinal neoplasms. *Int J Cancer*. 2017;140(4):853–863.